Proceedings of the ASME 2020 International Technical Conference and Exhibition
on Packaging and Integration of Electronic and Photonic Microsystems
InterPACK2020
October 27-29, 2020, Virtual, Online

IPACK2020-2595

CFD SIMULATION OF TWO-PHASE IMMERSION COOLING USING FC-72 DIELECTRIC FLUID

Amirreza Niazmand[1], Tushar Chauhan[2], Satyam Saini[3]
Pardeep Shahi[4], Pratik Vithoba Bansode[4], Dereje Agonafer[5]
University of Texas at Arlington
701 S. Nedderman Drive
Arlington, TX, USA

ABSTRACT

With more development in electronics system capable of having larger functional densities, power density is increasing. Immersion cooling demonstrates the highest power usage efficiency (PUE) among all cooling techniques for data centers and there is still interest in optimizing immersion cooling to use it to its full potential. The aim of this paper is to present the effect of inclination and thermal shadowing on two-phase immersion cooling using FC-72. For simulation of boiling, the RPI (Rensselaer Polytechnic Institute) wall boiling model has been used. Also, two empirical models were used for calculation of bubble departure diameter and nucleate site density. The boundary condition was assumed to be constant heat flux and the bath temperature was kept at boiling temperature of FC-72 and the container pressure is assumed to be atmospheric. this study showed that due to the thermal shadowing, boiling boundary layer can lay over the top chipset and increases vapor volume fraction over top chipsets. This ultimately causes increase in maximum temperature of second chip. The other main observation is with higher inclination angle of chip, maximum temperature on the chip decreases up to 3°C.

Keywords: Nucleate boiling, two-phase, immersion cooling of electronics, FC-72

INTRODUCTION

The demands for high performance computer (HPC) and supercomputers are dramatically increasing, and it is expected to reach near to exa-scale level of performance. As the performance and capacity of these devices increase, the heat which should be removed also increases. Between all components in a server, the CPUs and GPUs are the highest power components which need to be cooled down to the thermal design temperature to keep away from component failure.

Air cooling is extensively used for cooling of electronics devices. The fan blows air through hot components and it absorbs heat. The hot air is collected in ceiling through ducts. This air is then cooled down by other systems like air handling units or chillers and reinjected back to components through ducts and perforated floor. The limitation of using air for high-power system is that the air has low thermal properties and it means to remove more heat from the components, with this it requires larger mass flowrate and higher velocity which increase the energy consumption [2]. Figure 1 shows the PUE of different methods of cooling used in data center cooling.

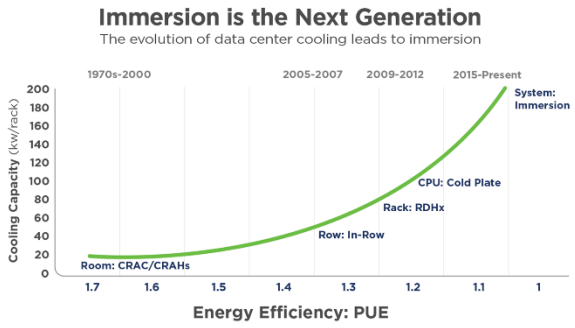

Figure 1: Cooling approaches: Efficiency vs Density [3]

For higher power density, which could not be cooled with air cooling, next available technology is indirect liquid cooling. Indirect liquid cooling uses cold plate, mounted on the active chip to absorb heat. Liquid coolant is circulated through cold plates, which absorbs and carries heat to heat exchanger and ultimately is dissipated to ambience. Dynamic cold plates could be used to control and regulate the flow rate distribution to hot

[1] Contact author: amirreza.niazmand@mavs.uta.edu

spot on multi-chip module and further push the capability and make it efficient [2].

Capabilities of air cooling could be expanded by adding in row cooler and rear door heat exchanger up to approximately 35 kW per rack. For higher power density, from 35-60 kW per rack approximately, indirect liquid coiling is dominant cooling method for data centers. Beyond this power density per rack, direct liquid cooling needs to be implemented. Direct liquid cooling also known as immersion cooling and classified into two major categories, single phase immersion cooling and two-phase immersion cooling [1].

In immersion cooling, high-energy electronic systems are immersed in dielectric liquid which its dielectric constant is smaller than water therefore they are safe for electronic systems. These liquids have better thermal properties compare to air. Thus, they can help us to keep the systems below their temperature limit with lower velocities which reduce the friction and energy consumption. Based on the boiling temperature and occurrence of phase change, immersion cooling can be divided in two categories of single and two-phase, which in single-phase, the coolant stays in liquid form but in two-phase, the liquid can boil in contact with the hot surface of electronic devices however this concept is not new and it is being used in many industries[[1]-[4]]. The high latent heat of vaporization helps heat to be extracted rapidly while the temperature of coolant stays almost constant.

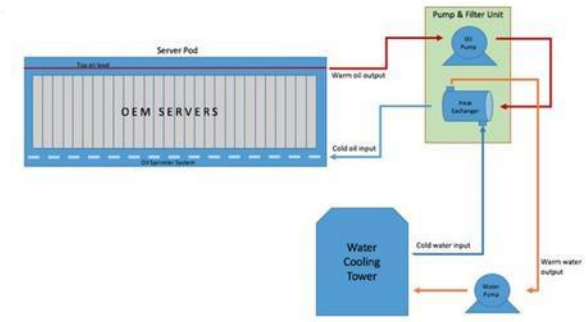

Figure 2: Schematic diagram for single phase immersion cooling [5]

In single phase immersion cooling, electronic systems are immersed into the dielectric coolant. Coolant carries heat and being circulated through heat exchanger. From heat exchanger, heat is ultimately rejected to ambient with cooling tower. Figure 3 shows the different part of single-phase cooling system. For single phase research, many scientists used fluorocarbon fluid or oil as a coolant in their systems. Eiland et. al used oil and dielectric liquid for cooling of a server to check different environmental operating conditions. They found that using oil compare to air can reduce the thermal resistance up to 34%[6]. In another research, the comparison of natural convection and force convection were studied to find a hot spot in the system [7], [8]. Although, the immersion cooling has good pay off from thermal point of view, it can damage or reduce the lifetime of the servers. Shah et. al investigated the equipment reliability and enhancements of reliability in data center when mineral oil is used as dielectric fluid. They check the effect of oil on many electronic parts like PVC, PCB and switches. They found that the oil can have degradation effect on some equipment like capacitors [9].

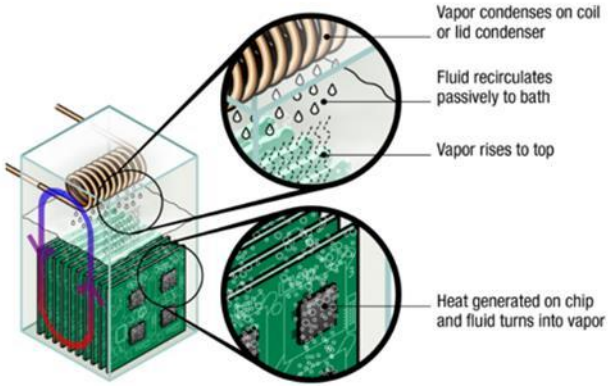

Figure 3: Schematic diagram for two-phase immersion cooling [10]

In two-phase immersion cooling, electronic system is immersed in dielectric fluid, as the temperature of the chip goes beyond saturation temperature of the fluid, it changes its phase from liquid to vapor. Vapor having lower density compared to liquid travel to the top of the tank. Accumulated vapor is condensed with condenser by removing heat from vapor, which changes its phase back to liquid and return to liquid sump due to gravity.

Tantolin et. al investigated the two-phase thermal performance of power components float in the liquid. They used a semi-conductor stack as the power source and the outer surface of test container was covered by fins. The air could pass through the fins to cool down the vapor inside the system. They discovered that the best performance happens when the filling ratio is near 80% [11]. Nguyen et al numerically studied the flow boiling in multichip modules. They used Novec 649 as the dielectric liquid and they studied different bubble departure diameter and site nucleation density to find the performance of each model in simulation of the system [12].

The objective of this paper is to investigate the effect of inclination and thermal shadowing for two-phase immersion cooling of a high energy chipsets. A numerical model was developed in ANSYS Fluent and the FC-72 was selected as liquid coolant that has medium boiling point (56^{o}C) and moderate latent heat of vaporization (88 kJ/kg) [13]. Effect of inclination was studied by changing of the gravity vector and three different angles were studied and the effect of shadowing was studied.

MATHEMATICAL MODELING

To simulate subcooled boiling, the Non-equilibrium model is used. Subcooled boiling is a kind of boiling that the bulk fluid temperature is less or equal to the boiling temperature, but the wall temperature is high enough to make boiling to happen. At first, the liquid gains energy to reach the boiling condition and after that the liquid starts to change phase however the temperature of liquid stays fixed but the temperature of vapor

can be changed due to energy transfer from the wall. Since boiling is a very complicated phenomenon, the energy also can be transferred between phase like transferring energy from the high temperature vapor to the liquid [14]. This can change the vapor quality and temperature in the area even far from the wall too.

The first equation that needs to be solved is continuity equation. All equations for RPI method need to be solved separately for each phase [15].

$$\frac{\partial}{\partial t}(\alpha_i \rho_i) + \nabla.(\alpha_i \rho_i \vec{v}_i) = \sum_{j=1}^{n} \dot{m}_{ij} - \dot{m}_{ji} \quad (1)$$

Where α is the mass fraction of each phase, ρ is the density of that phase that can be function of temperature and pressure and , j and i show the phase of fluid, liquid or vapor. $\vec{v}_i$ represents the velocity of that phase and $\dot{m}_{ij}$ depicts the mass transfer from phase i to j and $\dot{m}_{ji}$ depicts the mass transfer from phase j to i.

The momentum equation for boiling flow is defined as

$$\frac{\partial}{\partial t}(\alpha_i \rho_i \vec{v}_i) + \nabla.(\alpha_i \rho_i \vec{v}_i \vec{v}_i) = \alpha_i \nabla \mathrm{p} + \nabla.\bar{\bar{\tau}}_i + \alpha_i \rho_i g + \sum_{j=1}^{n} \vec{R}_{ij} + \dot{m}_{ij}\vec{v}_{ij} - \dot{m}_{ji}\vec{v}_{ji} + \vec{F}_i \quad (2)$$

Where $\vec{R}_{ij}$ shows the force of interaction between phases and $\vec{F}_i$ represents the forces includes external body force, lift force, wall lubrication force, virtual mass force and turbulent dispersion force. In addition, p is the pressure, $\bar{\bar{\tau}}_i$ is phase stress-strain tensor and g are the gravity.

For the reason that the boiling is a phase change phenomenon, the typical energy equation cannot be solved in this case. the formal energy equation includes heat capacity that is not meaningful while changing of phase happens therefore the energy equation should be solved based in the form of enthalpy. This form is capable of simulating the effect of changing phase. Accordingly, the energy equation for each phase can be written

$$\frac{\partial}{\partial t}(\alpha_i \rho_i h_i) + \nabla.(\alpha_i \rho_i \vec{v}_i h_i) = \alpha_i \frac{dp_i}{dt} + \bar{\bar{\tau}}_i : \nabla \vec{v}_i + \nabla.q_i + \sum_{j=1}^{n} Q_{ij} + \dot{m}_{ij}h_{ij} - \dot{m}_{ji}h_{ji} \quad (3)$$

Where h_i is the enthalpy of i phase, q_i is the heat flux and Q_{ij} is the intensity of heat exchange between phase i and j. h_{ij} characterizes the enthalpy transfer from phase i to j and h_{ji} characterizes the enthalpy transfer from phase j to i.

Generally boiling is turbulent phenomena and to simulate it the turbulent equation should be solved along other equations. the most suitable turbulent model for industrial cases is Reynolds Averaging Navier-Stocks model (RANS)[3], [4]. Amongst RANS models, $k-\omega$ model has good precision and stability. Therefore, for the present work, this model was selected. The basic idea of this model is to find the distribution of turbulence kinetic energy (k) and specific rate of dissipation (ω) in the domain through solving transport equation of each parameter.

$$\frac{\partial}{\partial t}(\alpha_i \rho_i k_i) + \nabla.(\alpha_i \rho_i \vec{v}_i k_i) = \nabla.\left(\alpha_i \mu_{eff} \nabla k_i\right) + S_i^k \quad (4)$$

$$\frac{\partial}{\partial t}(\alpha_i \rho_i \omega_i) + \nabla.(\alpha_i \rho_i \vec{v}_i \omega_i) = \nabla.\left(\alpha_i \mu_{eff} \nabla \omega_i\right) + S_i^\omega \quad (5)$$

The concept of RPI is based on the dividing the total wall heat flux to three main parts, the convective heat flux, the quenching heat flux and the evaporative heat flux.

$$\dot{q}_W = \dot{q}_C + \dot{q}_Q + \dot{q}_E \quad (6)$$

The convective heat flux $\dot{q}_C$ is defined as

$$\dot{q}_c = h_C(T_w - T_l)(1 - A_b) \quad (7)$$

Where A_b is expressed as area of influence where occupied by nucleating bubbles, thus $(1 - A_b)$ is the portion of wall surface which is not covered by fluid. h_C represents single phase heat transfer coefficient, and T_w and T_l show the wall and liquid temperature respectively.

The definition of are influence is

$$A_b = \min\left(1, K\frac{N_w \pi D_w^2}{4}\right) \quad (8)$$

Where N_w is nucleate site density, K is the empirical constant and usually is assumed to be "4" [5]. The D_w is departure diameter of bubbles from the surface. This form of Area of Influence equation helps to avoid numerical instabilities which occurs caused by unbound empirical correlations of nucleate site density equation[5]. The K can be calculated by

$$K = 4.8e^{\left(-\frac{Ja_{sub}}{80}\right)} \quad (9)$$

Where Ja_{sub} is subcooled Jacob number and is defined as

$$Ja_{sub} = \frac{\rho_l C_{p_l} \Delta T_{sub}}{\rho_v h_{fv}} \quad (10)$$

Where ρ_l is density of sub-cooled liquid, ρ_v is vapor density, C_{p_l} is sub-cooled liquid specific heat capacity.

The quenching heat flux ($\dot{q}_Q$) is defined as energy transfer when the liquid fills the wall vicinity after detachment of the bubble, and it is calculated by

$$\dot{q}_Q = \frac{2k_l}{\sqrt{\pi \lambda_l T}}(T_w - T_l) \quad (11)$$

Where λ_l is the thermal diffusivity and T is the periodic time. λ_l is expressed as

$$\lambda_l = \frac{k_l}{\rho_l C_{p_l}} \quad (12)$$

The last flux term in the RPI model is called evaporative flux ($\dot{q}_E$) and it is expressed by

$$\dot{q}_E = N_w V_d \rho_v h_{fv} \quad (13)$$

Where N_w represent nucleation site density, V_d is the volume of the bubble, ρ_v is the density of vapor and h_{fv} represents the latent heat of the vaporization.

Nucleate site density is one of the most important parameter in the simulation of boiling and for the present study, Kocamustafaogullari and Ishii [6] model is used for prediction of nucleate site density, which includes an empirical correlation which is given by

$$N_w^* = f(\rho^*) r_c^{*-4.4} \quad (14)$$

In this empirical formula, the parameters are defined as

$$N_w^* = N_w D_w^2 \quad (15)$$

$$r_c^* = 2r_c / D_w \quad (16)$$

$$\rho^* = (\rho_l - \rho_v)/\rho_v \quad (17)$$

Where D_w is wall departure diameter and r_c is given by

$$r_c = \frac{2\sigma T_{sat}}{\rho_v h_{fv} \Delta T_w} \quad (18)$$

In this formula, the σ represents surface tension, T_{sat} shows the saturation temperature of the fluid which can be function of pressure if the pressure change in the case is not negligible. ΔT_w depicts the difference between the wall temperature and the fluid temperature. Finally, the function $f(\rho^*)$ is given by

$$f(\rho^*) = 2.157 \times 10^{-7} \rho^{*-3.2} (1 + 0.0049\rho^*)^{4.13} \quad (19)$$

In most boiling cases, an empirical model is used to calculate bubble departure dimeter like Kocamustafaogullari and Ishii[7] or Unal[8] but in this case, research shows that the bubble departure diameter is now function of wall temperature difference and surface tension and as long as the boiling regime is nucleate boiling, the bubble departure diameter is constant and equal to 0.1mm [9].

SIMULATION SETUP AND BOUNDARY CONDITIONS

For this study, the FC-72 was chosen which has latent heat vaporization about 88 J/g while the boiling happens at atmospheric pressure and boiling temperature of 56^{O}C. The increase in working pressure is not recommended due to increase of boiling temperature which can damage the electronic components. Table 1 shows the properties of FC-72 for the two phases of liquid and vapor.

Figure 4 and Figure 7 show the boundary conditions for the validation case and the test case. These cases include one or two processors which are modeled by a uniform heat flux boundary condition. for the test cases, the heater is simulated to the wall by 2 mm space to consider the real thickness of processors. The size of processor for the validation test is 9mm by 9mm and the container is 200mm x 200mm x 500mm. for the test case, the processor size is 40mm x 40mm and the container dimension is 320mm x 200mm x 50mm. the space between the two processor for the double chips case is 40mm. all sides of containers, except one, is assumed to be closed wall and to be in insulated thus the zero-heat flux was used as boundary conditions. The top side of each container was assumed to be open and the pressure outlet boundary condition was chosen which let the flow enters and exits from the boundary. This condition allows the vapor, or the liquid leaves the container due to the buoyancy and allows the liquid comes back to the domain. In the real case, the vapor goes up and by contacting a condenser, it gets cooled and the saturated or subcooled liquid comes back to the domain but for the simulation, because of limitation in boiling model and computational resources, it is substituted by the opening boundary condition. The exit flow satisfies zero-gradient condition and for the inlet flow, the pressure is ambient pressure, but the temperature was set based on the temperature difference with saturation temperature which helps us to simulate the subcooled boiling in our case where it was set as one degree difference.

Table 1: Thermal properties of FC-72 at boiling temperature **[10]**

	Properties	**Value**
liquid	Average Molecular Weight	338
	Boiling Point (1 atm)	56°C
	Latent Heat of Vaporization	88 J/g
	Liquid Density	1680 kg/m^3
	Kinematic Viscosity	0.38 centistokes
	Absolute Viscosity	0.64 centipoise
	Liquid Specific Heat	1100 J kg^{-1} C^{-1}
	Liquid Thermal Conductivity	0.057 W m^{-1} °C^{-1}
Vapor	vapor Density	13.1 kg/m^3
	Kinematic Viscosity	0.1 centistokes
	Absolute Viscosity	0.124 centipoise
	Vapor Specific Heat	900 J kg^{-1} C^{-1}
	Vapor Thermal Conductivity	0.0235 W m^{-1} °C^{-1}

RESULT AND DISCUSSION

To validate wall boiling model, an experimental case with simple geometry is chosen and the result of numerical simulation is compared to the experimental result to see the performance of the model. Therefore, an experimental with FC-72 as liquid is selected[11]. The experimental includes a chamber with a single chip at the bottom of the chamber to find the boiling characteristic curve. The size of chip is 9x9 mm and the surroundings of the chip is kept far from the chip to make sure that the other walls cannot affect the results.

shows the geometry of chamber used for numerical simulation and validation case.

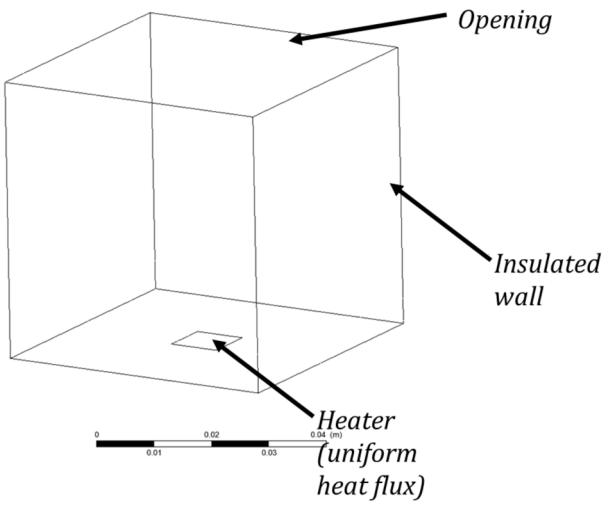

Figure 4: the chamber geometry for validation case and boundary conditions

For this study, FC-72 properties are used. FC-72 is one of the fluorocarbons which is widely used in experiments and industrial cases for the purpose of the two-phase cooling. shows the properties of FC-72 at the temperature of 55°C and atmospheric pressure. For the vapor, properties are function of temperature and pressure due to lack of data for the vapor properties, a nonlinear equation of state is used for calculation and the calculated properties later was imported as table to the software for simulation.

This geometry was simulated for 3 different grid numbers from 800k to 2.5M to be sure that the numerical error due to spatial discretization is minimum and the error of average temperature of the surface reaches to less than 1 percent and the convergence criteria was set to $1e^{-6}$ for all variables. To increase the stability of solution, all relaxation factor was set to 0.1 and the multigrid method was used.

Figure 5**Error! Reference source not found.** shows the isosurface of 10% vapor volume fraction colored by the velocity of vapor phase. As it shows, the bubble start to rise from the surface of the heat source and goes up due to gravity forces. Because of the natural convection flow inside the chamber, the bubbles tend to gather in the midline of the chamber. Figure 6 shows the saturation boiling curve of validation case. this curve shows that as heat flux increases the difference between wall temperature and saturation temperature also increases. The current simulation just covers the nucleation boiling regime which is up to 15 W/cm^2.

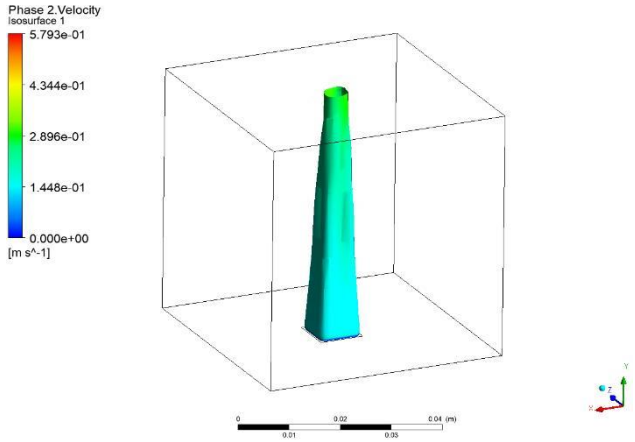

Figure 5: Isosurface of 10% vapor volume fraction colored by the velocity

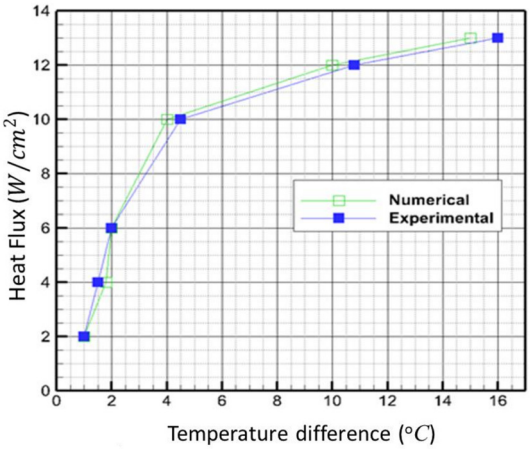

Figure 6: saturation boiling curve of FC-72 for validation case

In this paper, two-phase immersion cooling for single and double chipset are studied for FC-72 as coolant. The ambient temperature and temperature of liquid are kept at 56°C which is the boiling temperature of the FC-72. The chipset size for all cases are 4cmx4cm that is close to all CPU sizes. The cases are simulated for different inclination and for a variety of power. In this case the pressure is kept at atmospheric pressure. The properties which are used for simulation are depicted in Table 1. Figure 7 describes the boundary condition used for this simulation.

Figure 8 depicts the isosurface of 10% volume fraction of vapor over two chipsets. As it shows, the boundary layer starts from the bottom chipsets and it tends to the center line of the chipset and it covers the center area of top chipsets. The top chipset also has boiling boundary layer therefore, the boundary layer starts to grow from both sides of the top chipset.

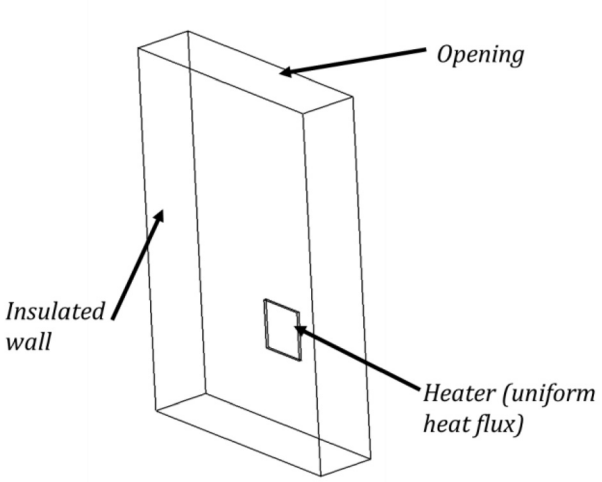

Figure 7: Domain geometry and Boundary conditions

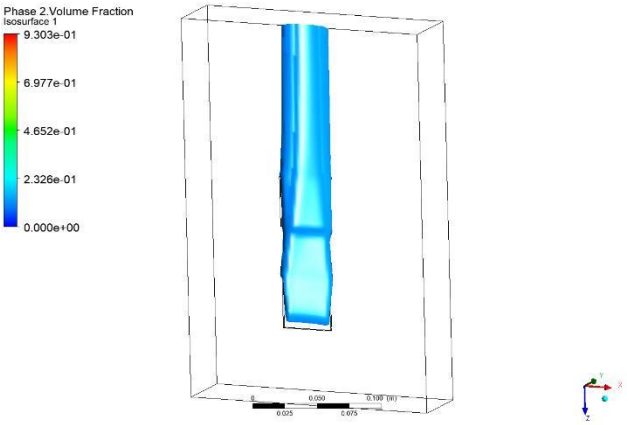

Figure 8: Isosurface of vapor volume fraction over chipsets

Figure 9 shows the distribution of vapor volume fraction over the chipsets. The bottom figure shows the case which the power of chipset is 4 W/cm^2. In this case most of area of the bottom chipset is covered by the liquid and at the top of the bottom chipset it starts boiling but for the top chipset, it is covered by the vapor except two narrow band at the left and right of the chipset which has contact with liquid. the top figure shows the case which the power is 15 W/cm^2. For this case, the boiling starts from the middle chipset and the quality of vapor will reach about 0.25. the top chipset is fully covered by the vapor and on the top of this chipset the quality of the vapor reaches about the 0.93.

Figure 10 shows the effect of inclinations on the boiling curve. The general pattern for all curves is the same but the curve is shifted to the left which is the effect of inclination. It shows that by changing the inclination, the temperature difference reduces due to penetration of liquid over the chipset surfaces. Also, the curves are diverging for higher heat fluxes and as heat flux increases, the temperature difference also increases.

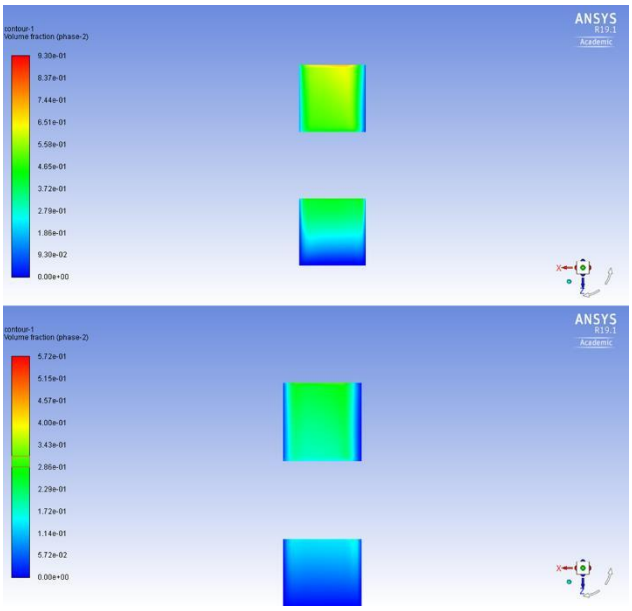

Figure 9:distribution of volume fraction over the chipsets (bottom:4W/cm2, top:15W/cm2).

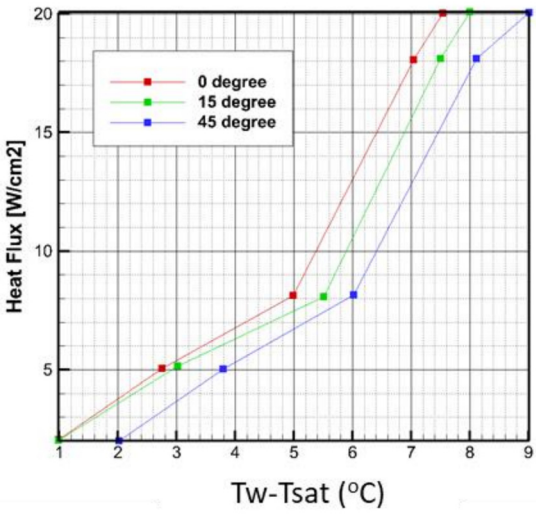

Figure 10: Effects of different inclinations on simulated boiling curves of the bottom chipsets

CONCLUSION

This work investigated two-phase immersion cooling for two chipsets. The FC-72 was selected as working liquid and the properties of liquid were used as constant but for the gas form, the properties were calculated based on the nonlinear ideal gas. The two chipsets were placed in series to study the effect of thermal shadowing. The chipsets were in a container with one opening and the temperature of ambient were assumed to be constant and for the whole case, it is assumed that pressure is constant and equal to atmospheric pressure. To be sure about the accuracy of the results, a standard case was simulated, and the

results were compared to the experimental result which agrees well with experimental results.

REFERENCES

[1] X. An, M. Arora, W. Huang, W. C. Brantley, and J. L. Greathouse, "3D Numerical Analysis of Two-Phase Immersion Cooling for Electronic Components," in *2018 17th IEEE Intersociety Conference on Thermal and Thermomechanical Phenomena in Electronic Systems (ITherm)*, 2018, pp. 609–614, doi: 10.1109/ITHERM.2018.8419528.

[2] S. V Patankar, "Airflow and Cooling in a Data Center," *J. Heat Transf.*, vol. 132, no. 7, pp. 73001–73017, Apr. 2010.

[3] grccooling, "Liquid Immersion Cooling for Data Centers," 03-Jul-2019. [Online]. Available: https://www.grcooling.com/ 0.

[4] J. Fathi Sola, F. Alinejad, F. Rahimidehgolan, and A. Niazmand, "Fatigue life assessment of crankshaft with increased horsepower," *Int. J. Struct. Integr.*, vol. 10, no. 1, pp. 13–24, Jan. 2019, doi: 10.1108/IJSI-04-2018-0020.

[5] Submer, "What is Immersion Cooling?," 03-Jul-2019. [Online]. Available: https://submer.com/blog/what-is-immersion-cooling 0.

[6] R. Eiland, J. Edward Fernandes, M. Vallejo, A. Siddarth, D. Agonafer, and V. Mulay, "Thermal Performance and Efficiency of a Mineral Oil Immersed Server Over Varied Environmental Operating Conditions," *J. Electron. Packag.*, vol. 139, no. 4, pp. 41005–41009, Sep. 2017.

[7] L. W. Pierce, "An investigation of the thermal performance of an oil filled transformer winding," *IEEE Trans. Power Deliv.*, vol. 7, no. 3, pp. 1347–1358, 1992, doi: 10.1109/61.141852.

[8] A. Niazmand, J. Fathi Sola, F. Alinejad, and F. Rahimi Dehgolan, "Investigation of Mixed Convection in a Cylindrical Lid Driven Cavity Filled with Water-Cu Nanofluid," *Inventions*, vol. 4, no. 4, 2019, doi: 10.3390/inventions4040060.

[9] J. M. Shah, R. Eiland, A. Siddarth, and D. Agonafer, "Effects of mineral oil immersion cooling on IT equipment reliability and reliability enhancements to data center operations," in *2016 15th IEEE Intersociety Conference on Thermal and Thermomechanical Phenomena in Electronic Systems (ITherm)*, 2016, pp. 316–325, doi: 10.1109/ITHERM.2016.7517566.

[10] Allied Controls, "https://www.allied-control.com/the-basics-of-immersion-cooling," 2018. [Online]. Available: https://www.allied-control.com/the-basics-of-immersion-cooling 0.

[11] C. Tantolin, M. Lallemand, and U. Eckes, "Experimental study of immersion cooling for power components," in *1994 International Conference on Control - Control '94.*, 1994, vol. 1, pp. 723–727 vol.1, doi: 10.1049/cp:19940221.

[12] J. Nguyen *et al.*, "A Numerical Study of Multiphase Dielectric Fluid Immersion Cooling of Multichip Modules Including Effects of Nucleation Site Density and Bubble Departure Diameter Functions," no. 57496. p. V08AT10A032, 2015.

[13] M. S. El-Genk and J. L. Parker, "Nucleate boiling of FC-72 and HFE-7100 on porous graphite at different orientations and liquid subcooling," *Energy Convers. Manag.*, vol. 49, no. 4, pp. 733–750, 2008, doi: https://doi.org/10.1016/j.enconman.2007.07.028.

[14] T. Ren, C. Yan, M. Yan, and S. Yu, "CFD Analysis on Wall Boiling Model During Subcooled Boiling in Vertical Narrow Rectangular Channel," no. 51524. p. V008T09A016, 2018.

[15] B. G. Dehkordi, S. Fallah, and A. Niazmand, "Investigation of harmonic instability of laminar fluid flow past 2D rectangular cross sections with 0.5-4 aspect ratios," *Proc. Inst. Mech. Eng. Part C J. Mech. Eng. Sci.*, vol. 228, no. 5, pp. 828–839, 2014, doi: 10.1177/0954406213491906.

[16] B Ghadiri Dehkordi, A Niazmand, and S Soheili, "Study the Consistency of k-ε and Smagorinsky Models in Simulation of Circular Cylinder," in *The 10th Iranian Aerospace Society Conference*, 2011.

[17] Amirreza Niazmand, "Large eddy simulation of internal incompressible turbulent flow using structure sub-grid eddy viscosity model in a lid driven cavity," 2011.

[18] V. H. Del Valle and D. B. R. Kenning, "Subcooled flow boiling at high heat flux," *Int. J. Heat Mass Transf.*, vol. 28, no. 10, pp. 1907–1920, 1985, doi: https://doi.org/10.1016/0017-9310(85)90213-3.

[19] G. Kocamustafaogullari and M. Ishii, "Foundation of the interfacial area transport equation and its closure relations," *Int. J. Heat Mass Transf.*, vol. 38, no. 3, pp. 481–493, 1995, doi: https://doi.org/10.1016/0017-9310(94)00183-V.

[20] G. Kocamustafaogullari and M. Ishii, "Interfacial area and nucleation site density in boiling systems," *Int. J. Heat Mass Transf.*, vol. 26, no. 9, pp. 1377–1387, 1983, doi: https://doi.org/10.1016/S0017-9310(83)80069-6.

[21] H. C. Unal, "Maximum bubble diameter, maximum bubble-growth time and bubble-growth rate during the subcooled nucleate flow boiling of water up to 177 MN/m2," *Int. J. Heat Mass Transf.*, vol. 19, no. 6, pp. 643–649, 1976.

[22] B. B. Mikic and W. M. Rohsenow, "A New Correlation of Pool-Boiling Data Including the Effect of Heating Surface Characteristics," *J. Heat Transf.*, vol. 91, no. 2, pp. 245–250, May 1969.

[23] R.-H. C. Daniel P. Rini Louis C. Chow, "BUBBLE BEHAVIOR AND HEAT TRANSFER MECHANISM IN FC-72 POOL BOILING," *Exp. Heat Transf.*, vol. 14, no. 1, pp. 27–44, Jan. 2001, doi: 10.1080/089161501461620.

